Journal of Photochemistry and Photobiology A: Chemistry 220 (2011) 153–163

Contents lists available at ScienceDirect

Journal of Photochemistry and Photobiology A: Chemistry

journal homepage: www.elsevier.com/locate/jphotochem

A Schiff base-derived new model compound for selective fluorescence sensing of Cu(II) and Zn(II) with ratiometric sensing potential: Synthesis, photophysics and mechanism of sensory action

Bijan Kumar Paul, Samiran Kar, Nikhil Guchhait*

Department of Chemistry, University of Calcutta, 92 A. P. C. Road, Calcutta 700009, India

ARTICLE INFO

Article history:
Received 19 January 2011
Received in revised form 10 March 2011
Accepted 4 April 2011
Available online 13 April 2011

Keywords:
Fluorescence chemosensor
Ratiometric sensing
Cu(II) ion
Zn(II) ion
Photoinduced electron transfer (PET)

ABSTRACT

A new Schiff base compound 2-[(naphthalen-1-ylmethylimino)-methyl]-naphthalen-1-ol (2N1YMN1O) has been synthesized and characterized by ^{1}H NMR, ^{13}C NMR, DEPT, and FT-IR spectroscopy. A spectral deciphering of the photophysics of 2N1YMN1O has been undertaken by stationary absorption, emission and time-resolved emission techniques. A significantly low fluorescence yield of the compound has been realized in connection with photo-induced electron transfer (PET) to the naphthalene fluorophore unit from the imine receptor moiety. Subsequently, an assay for the transition metal ion-induced modulation of the fluorophore-receptor communication reveals the promising prospect of 2N1YMN1O to function as a fluorosensor for Cu^{2+} and Zn^{2+} ions selectively, through noticeable fluorescence enhancement. While perturbation of Cu^{2+}/Zn^{2+} ion-induced PET in 2N1YMN1O has been argued to be the operating mechanism behind the fluorescence enhancement, the selectivity for these two metal ions has been interpreted on the grounds of an appreciably strong binding interaction. Particularly noticeable aspects regarding the chemosensory activity of the compound are: (i) its selectivity for Cu^{2+} and Zn^{2+} ions, (ii) ratiometric sensing potential, (iii) the construction of a calibration curve for detection of Cu^{2+} and Zn^{2+}, (iv) ability to detect the transition metal ions down to the level of micromolar concentration, (v) a simple synthetic route, (vi) exploring the function of an imine nitrogen as a receptor unit in the proposed PET mechanism.

© 2011 Elsevier B.V. All rights reserved.

1. Introduction

Molecular systems that perform specific light-induced logic operations have drawn considerable attention since years [1–7]. This is obvious because of their viable application in the development of molecular switches and information storage devices at the molecular level [8–11]. Apart from these, the strategy of simple switching of light between “OFF” and “ON” states underlies the potential for development of signaling systems by responding to the presence of an analyte [12].

In a general sense, a chemosensor is referred to a compound that displays significant modulation of its signaling observable upon interaction with the guest counterpart. Though, the observable signal may, in principle, range in being electrical, electronic, magnetic, optical, pH-metric and so forth, an architecture based on fluorescence signaling promises to have additional edges. This is related to the specificity, sensitivity, real time monitoring with fast response time and cost-effectiveness of the technique [13–15]. The strategy of fluorescence intensity modulation upon binding to species of interest has formed the foundation of the working concept for many reported fluorescence sensors [15–19]. However, ratiometric sensing scheme is more fruitful as an actuating tool since it is independent of experimental and instrumental artifacts like fluctuations in probe concentration, excitation source intensity, light scattering, stability under illumination, environment around the sensor molecule (medium pH/polarity, temperature, pressure, etc.) and so forth, and hence is independent of the need of frequent calibration during estimation of the analyte [13,14,20,21].

On the other extreme, sensing of transition metal ions has long been realized as an important goal in chemistry and biology [1,22,23]. Transition metals have been central in these perspectives with a view to their important biological and environmental roles [24–26].

Zinc is the second most abundant transition metal ion in human body and is an essential co-factor in many biological processes like brain function and pathology, gene transcription, immune function, etc. [24,25]. Another biologically important trace metal ion is copper. Maintenance of the proper level of Cu^{2+} ion is crucial as an excess of it might lead to gastrointestinal disorder, or even kidney or liver damage [26].

* Corresponding author. Tel.: +91 33 2350 8386; fax: +91 33 2351 9755.
E-mail address: nguchhait@yahoo.com (N. Guchhait).

1010-6030/$ – see front matter © 2011 Elsevier B.V. All rights reserved.
doi:10.1016/j.jphotochem.2011.04.006

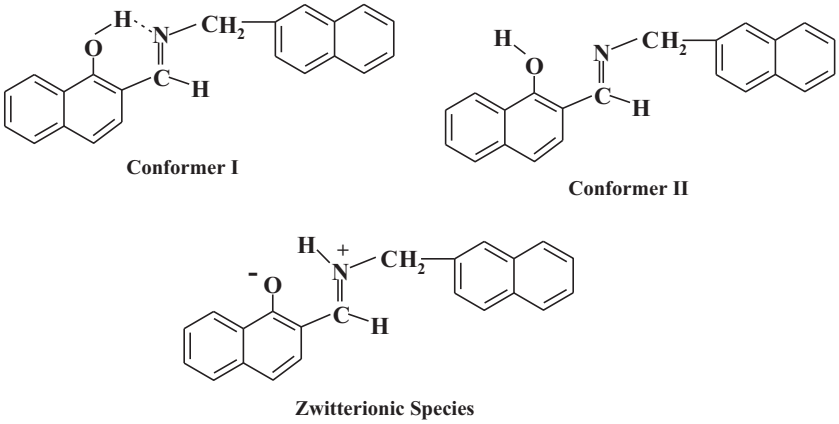

Scheme 1. Schematic of different conformers of 2N1YMN1O.

Thus considerable efforts have been dedicated to development of fluorescence chemosensor for these two transition metal ions [14,16–19,27,28]. The present work describes the synthesis, photophysical characterization of a Schiff base-derived new model compound viz, 2-[(Naphthalen-1-ylmethylimino)-methyl]-naphthalen-1-ol (2N1YMN1O, see Scheme 1). Transition metal ion-induced modification of its photophysics has subsequently been argued to be a promising avenue for the development of a new fluorescence chemosensor for Cu(II) and Zn(II). A detailed assessment over the range of first row transition metal ions and alkaline earth cations reveals the selectivity of 2N1YMN1O for Cu(II) and Zn(II). The mechanism of the sensory action has been rationalized in connection with PET mechanism. At the same time, the structural simplicity of the molecular system is worth noting, together with the remarkable simplicity of its synthetic procedure.

2. Experimental

2.1. Materials

The detailed synthetic procedure and purification of the Schiff base 2N1YMN1O is described in the supplementary information.

Spectroscopic grade acetonitrile (ACN) was purchased from Spectrochem, India and used after proper purification according to standard procedures. Further, from $E_T(30)$ measurements it was confirmed that the ACN used for spectroscopic study was almost free from moisture [29]. The solvent was found free from impurities and appeared transparent in the spectral region of interest. The purity was also verified by recording the emission spectra in the studied spectral region.

The metal salts used in the present investigation are as follows: $Zn(ClO_4)_2(H_2O)_6$, $CrCl_3(H_2O)_6$, $Cu(ClO_4)_2(H_2O)_6$, $Fe(ClO_4)_2(H_2O)_6$, $Ni(ClO_4)_2(H_2O)_6$, $Co(ClO_4)_2(H_2O)_6$. The metal salts were procured locally and used as received. Perchlorate salts have been preferred because of the low co-ordinating ability of the anion counterpart. However, experiments with nitrate and chloride salts of the metal ions are found to bring about no significant changes in the observations. Nevertheless, perchlorate salts are preferred for reasons stated above.

All other solvents and reagents such as methylcyclohexane (MCH), methanol (MeOH), heptane (HEP), cyclohexane (CYC), tetrahydrofuran (THF) were of spectroscopic grade (Spectrochem, India) and were used after proper distillation. Ethanol (EtOH) from E-Merck was used as supplied. Triple distilled water was used for preparing aqueous solutions. $CDCl_3$ and DMSO-*d6* used for NMR experiments were used as received from Sigma-Aldrich, USA.

2.2. Instrumentations and methods

2.2.1. Steady-state spectral measurements

The absorption and emission spectra were acquired on Hitachi UV-Vis U-3501 spectrophotometer and Perkin Elmer LS-50B fluorimeter, respectively. For all spectroscopic measurements, the 2N1YMN1O concentration was maintained at ca. 8×10^{-6} mol/dm^3 in order to avoid reabsorption and aggregation effects. Only freshly prepared solutions were used for spectroscopic measurements. All experiments have been carried out at ambient temperature (300 K) unless otherwise specified.

The effect of metal ions on the spectral characteristics of 2N1YMN1O was monitored by adding few microlitre amounts of the stock solution of the metal salts to a known volume of the solution of 2N1YMN1O in ACN (2.50 ml). The addition of metal ions was restricted within 100.00 μl so as to eliminate the possibility of any significant volume change.

For processing of all sorts of interpretations based upon fluorescence intensity data the necessary corrections for inner filter effect has been done according to the following equation [6,13]:

$$I = I_{obs} \times \exp\left[\frac{1}{2}(A_{ex} + A_{em})\right] \quad (1)$$

Here I is the corrected fluorescence intensity and I_{obs} is the observed background-subtracted fluorescence intensity of the sample under investigation. A_{ex} and A_{em} are the measured absorbance at the excitation and emission wavelengths, respectively.

2.2.2. Time-resolved fluorescence decay

Fluorescence lifetimes were obtained from time-resolved intensity decays by the method of Time Correlated Single-Photon counting (TCSPC) using nanoLED-07 (IBH, U.K.) as the light source at 340, and 405 nm to trigger the fluorescence of the sample under study. The decays were deconvoluted on data station v2.3 IBH DAS6 decay analysis software. The quality of the fits was evaluated from χ^2 criteria and visual inspection of the residuals of the fitted function to the data. Mean (average) fluorescence lifetime ($\langle\tau_f\rangle$) for the multiexponential decay was determined from the decay time constants (τ) and the pre-exponential factors (α) using the following equation [13]

$$\langle\tau_f\rangle = \frac{\sum_i \alpha_i \tau_i^2}{\sum_i \alpha_i \tau_i} \quad (2)$$

2.2.3. Cyclic voltametry

The voltametric measurements were performed with a Sycopel model AEW21820F/L instrument. The experiments were carried

Table 1
Spectroscopic parameters for 2N1YMN1O in various solvents as obtained from absorption and emission measurements.

Solvent	Absorption λ (nm)			Fluorescence λ (nm)[a]	Quantum yield, Φ_f[b]	f[c]
	λ_1	λ_2	λ_3			
MCH	270	365	430	480	0.18	26.11
THF	270	365	430	490	0.15	42
CCl_4	270	365	430	490	0.16	42
ACN	270	365	430	486	0.098	53.06
EtOH	268	365	430	490	0.12	46.67
MeOH	268	365	430	490	0.11	29.09

[a] λ_{ex} = 365 nm for nonpolar solvents and λ_{ex} = 430 nm for polar solvents.
[b] Quantum yields are $\times 10^{-2}$ order.
[c] The term f is the factor by which the fluorescence yield of 2N1YMN1O is lower than its parent compound, HN12.

out in a standard three-component cell equipped with a glassy carbon working electrode, a Pt wire as an auxiliary electrode and Ag/AgCl reference electrode. The cyclic voltagrams were acquired in a N_2-bubbled acetonitrile solution containing ~0.2 M tetraethylammonium perchlorate (TEAP) as supporting electrolyte. The scan speed was 50 mV/s.

2.2.4. NMR study

All NMR spectra are recorded with TMS as internal standard on Bruker, Advance 300, Digtal NMR system. The solvents used in NMR spectral study are mentioned in respective parts of the discussions.

3. Results and discussions

3.1. Photophysical characterization of 2N1YMN1O

3.1.1. Absorption study

The absorption spectra of 2N1YMN1O have been recorded in various solvents and are displayed in Fig. 1, with the corresponding spectroscopic parameters being summarized in Table 1. 2N1YMN1O exhibits three absorption bands viz. at ≈270 nm, ≈365 nm and ≈430 nm wavelength regions. For assignments of the spectral bands of 2N1YMN1O we contemplate the anticipation with the spectral properties of the parent compound 1-hydroxy-2-naphthaldehyde (HN12). HN12 exhibits two prominent absorption bands at ≈300 nm and ≈370 nm wavelength regions which are attributed to the open form and intramolecularly hydrogen bonded closed form of HN12, respectively [30]. That the closed form absorbs at lower energy region ($\lambda_{abs} \approx 370$ nm) is a manifestation of the greater degree of stability due to the presence of the intramolecular hydrogen bonding (IMHB) interaction. In direct analogy to the spectral features of the parent molecule (HN12) [30] and other similar studied systems [31–34], the ≈365 nm absorption band is ascribed to the intramolecularly hydrogen bonded lowest energy ground state conformer, i.e. conformer **I** (Scheme 1) and the higher energy band (≈270 nm) may be due to the open conformer (conformer **II** in Scheme 1). That conformer **I** absorbs in the lower energy region is a corroboration of the extra degree of stabilization out of the IMHB interaction.

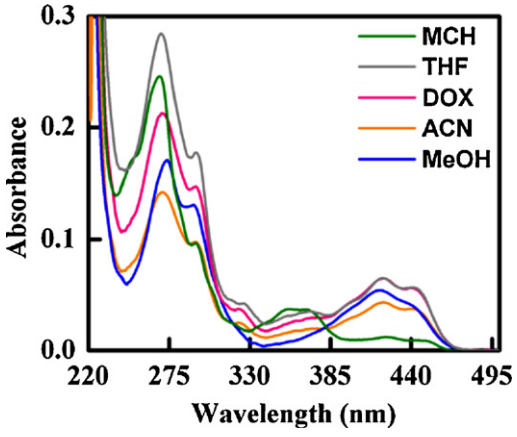

Fig. 1. Absorption spectra of 2N1YMN1O in different solvents as specified in the figure legend.

Though the assignment of the lowest energy absorption band ($\lambda_{abs} \approx 430$ nm) remains a matter of debate, a direct comparison with spectroscopic properties of structurally related compounds [31–34] tends to attribute the band to the zwitterionic species (Scheme 1). Also this observation seems to be self-authenticated by the fact that the zwitterionic species is capable of undergoing substantial stabilization through delocalization of its formal charges whence it absorbs in the lower energy region. Additionally, it is noteworthy at this stage that the absorption band for the zwitterionic species ($\lambda_{abs} \approx 430$ nm) gains a greater intensity compared to that for the closed form (i.e. conformer **I** in Scheme 1; $\lambda_{abs} \approx 365$ nm) in polar solvents, while the reverse pattern is noted in nonpolar solvent (Fig. 1). This is not surprising since the zwitterionic species (charge separated species) is expected to be more stabilized and hence more populated in polar solvents than in nonpolar solvents. Furthermore, it is seen that the absorption bands of 2N1YMN1O corresponding to the open ($\lambda_{abs} \approx 270$ nm) and closed ($\lambda_{abs} \approx 365$ nm) conformers are relatively blue shifted compared to those of the parent compound HN12 ($\lambda_{abs} \approx 300$ nm for the open form and $\lambda_{abs} \approx 370$ nm for the closed form [30]). This observation does not appear uncanny since the IMHB in 2N1YMN1O involving a weaker acceptor nitrogen should be weaker than that in HN12 involving a comparatively stronger acceptor oxygen.

3.1.2. Emission study

The emission spectra of 2N1YMN1O for λ_{ex} = 365 nm and 430 nm have been recorded in various solvents and the representative profiles obtained with λ_{ex} = 430 nm are illustrated in Fig. 2a, while the corresponding spectroscopic parameters are collected in Table 1. Excitation at either of the two wavelengths (viz., 365 nm and 430 nm) is found to produce emission maxima peaking at $\lambda_{em} \approx 490$ nm, which is thus subsequently ascribed to the emission coming from the locally excited state of the zwitterionic species (Scheme 1). Excitation at λ_{ex} = 365 nm also yields emission maxima at $\lambda_{em} \approx 490$ nm. This can be rationalized on the ground that the closed form of 2N1YMN1O undergoes a transformation to the zwitterionic form on the excited state potential energy surface prior to emission. Within the range of solvents assayed the emission maxima position is found to exhibit no noteworthy dependence on solvent polarity (Fig. 2a and Table 1). However, it is likely to consider the presence of more than one species (e.g. the closed conformer **I**, the open form (conformer **II**), the zwitterionic species, etc.) under the broad emission spectral profile [31–34]. The excitation spectra (Fig. 2b) are found to exhibit two bands at ≈295 nm and ≈428 nm along with a small hump at ≈370 nm, i.e.

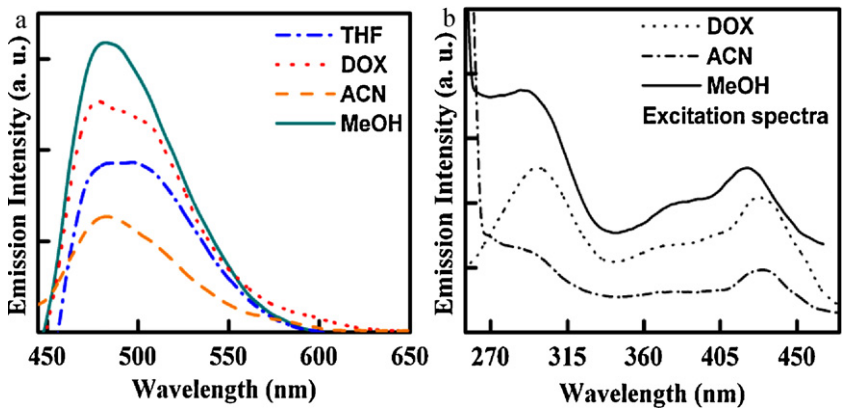

Fig. 2. (a) Emission (λ_{ex} = 365 nm) and (b) excitation ($\lambda_{monitored} = \lambda_{em}^{max}$) spectral profile of 2N1YMN1O in various solvents as specified in the figure legend.

the excitation spectral profile juxtaposes well with the absorption spectra.

3.1.3. Fluorescence quantum yields

The fluorescence quantum yields (Φ_f) of 2N1YMN1O in solvents of various polarities have been measured relative to recrystallized β-naphthol (Φ_f = 0.23 in MCH [13]) using the following equation [13]:

$$\Phi_f = \Phi_{std} \times \frac{(Abs)_{std}}{I_{std} \cdot \eta_{std}^2} \times \frac{I\eta^2}{Abs} \quad (3)$$

in which '*Abs*' is the absorbance, *I* is the fluorescence area under the curve, η is the refractive index of the medium. The subscript '*std*' stands for denoting the respective parameters for the secondary standard (β-naphthol).

The calculated values of quantum yields in different solvents are summarized in Table 1 and are found to be noticeably lower compared to those of its parent molecule HN12 [30]. The reason and consequence of such low fluorescence yields of the title compound will be further addressed and elaborated in forthcoming discussion.

3.2. Transition metal ion-induced modulation of photophysics of 2N1YMN1O

3.2.1. Steady-state spectral properties

In course of monitoring the effect of transition metal ions on the steady-state spectral properties of 2N1YMN1O, the absorption spectra is found to be hardly perturbed by the presence of the transition metal ions, as evident from Fig. 3. Only with Cu^{2+}, an exception could be noted (Fig. 3g). Gradual addition of Cu^{2+} ion to an ACN solution of 2N1YMN1O is found to accompany a decrease in absorbance at ≈430 nm with simultaneous emergence of a new band at ≈570 nm (Fig. 3g).

On the emission profile, however, transition metal ion-induced changes are more intriguing to note. No other metal ion, except Zn^{2+} and Cu^{2+}, is found to be able to impart any significant modulation to the emission characteristics of 2N1YMN1O, as evident from the results displayed in Fig. 4. On the other hand, Fig. 5 exhibits remarkable emission intensity enhancement of the studied compound in the presence of Zn^{2+} and Cu^{2+}. The insets of Fig. 5 illustrate that the excitation spectral profiles of 2N1YMN1O in the presence of the two metal ions (Zn^{2+} and Cu^{2+}) are not in agreement with the corresponding absorption spectra (*vide* Fig. 3f and g), indicating that the transition metal ion (Zn^{2+} and Cu^{2+})-induced modulation to the emission characteristics of 2N1YMN1O (*vide* Fig. 5) is an excited state affair. This observation has been further substantiated in the forthcoming discussion during elucidation of the mechanism of action of the transition metal ions.

Fig. 5c depicts the photographs showing visual colour changes of 2N1YMN1O in the presence of Zn^{2+} and Cu^{2+} ions. The solution of 2N1YMN1O in acetonitrile is found to undergo no significant change of colour in the presence of Zn^{2+} ion, whereas the presence of Cu^{2+} ion induces a prominent colour change. This result may hint at the prospective use of 2N1YMN1O to discriminate between the presence of Zn^{2+} and Cu^{2+} ions with the naked eyes.

3.2.2. Ratiometric chemosensory response of 2N1YMN1O

The foregoing discussions reveal Cu^{2+} and Zn^{2+} ion-induced modulation of spectroscopic properties of 2N1YMN1O, particularly on the emission profile. This observation subsequently leads to the concept of utilizing such transition metal ion-induced modulations of spectral response of 2N1YMN1O as a probable tool for exploiting the sensory action of the compound. The chemosensory emission spectral response of 2N1YMN1O to the series of first row transition metal ions is constructed on the basis of variation of relative fluorescence intensity of the compound (i.e. I/I_0 where I_0 and I are fluorescence intensities in the absence and presence of a defined amount of the transition metal ion, respectively) as a function of a defined concentration of the metal ions and is illustrated in Fig. 6a. The figure clearly advocates for the selective chemosensory response of 2N1YMN1O to Cu^{2+} and Zn^{2+} ions only. Furthermore, the selectivity of 2N1YMN1O for Cu^{2+} and Zn^{2+} ions has been tested against its response to alkaline earth metal ions, the presence of which was found to impart no significant modulation to the photophysical characteristics of 2N1YMN1O. Herein, we have emphasized on the exploration of ratiometric sensing scheme for reasons stated earlier.

Apart from such chemosensory response of 2N1YMN1O, the utilization of the ratiometric emission spectral response has been further extended to the construction of calibration curves for sensing of Cu^{2+} and Zn^{2+} ions. The variation of relative fluorescence intensity (I/I_0) of 2N1YMN1O over a range of metal ion concentration exhibits a fairly linear regression (Fig. 6b and c) whereby paving a way for estimation of Cu^{2+} or Zn^{2+} in an unknown sample utilizing the chemosensory property of the studied compound. It is also worth noting at this stage that the method based on chemosensory emission spectral response of 2N1YMN1O carries with it the promise of sensing transition metal ions (selectively Zn^{2+} and Cu^{2+}) up to a sufficiently low concentration, such as in the micromolar order (Fig. 6b and c). Also the calibration curves in Fig. 6b and c can be used to demarcate the response of 2N1YMN1O towards Cu^{2+} and Zn^{2+}.

3.2.3. Mechanism of sensory action of 2N1YMN1O

As already mentioned in Section 1, the mechanism of sensory action of the studied compound has been attempted to

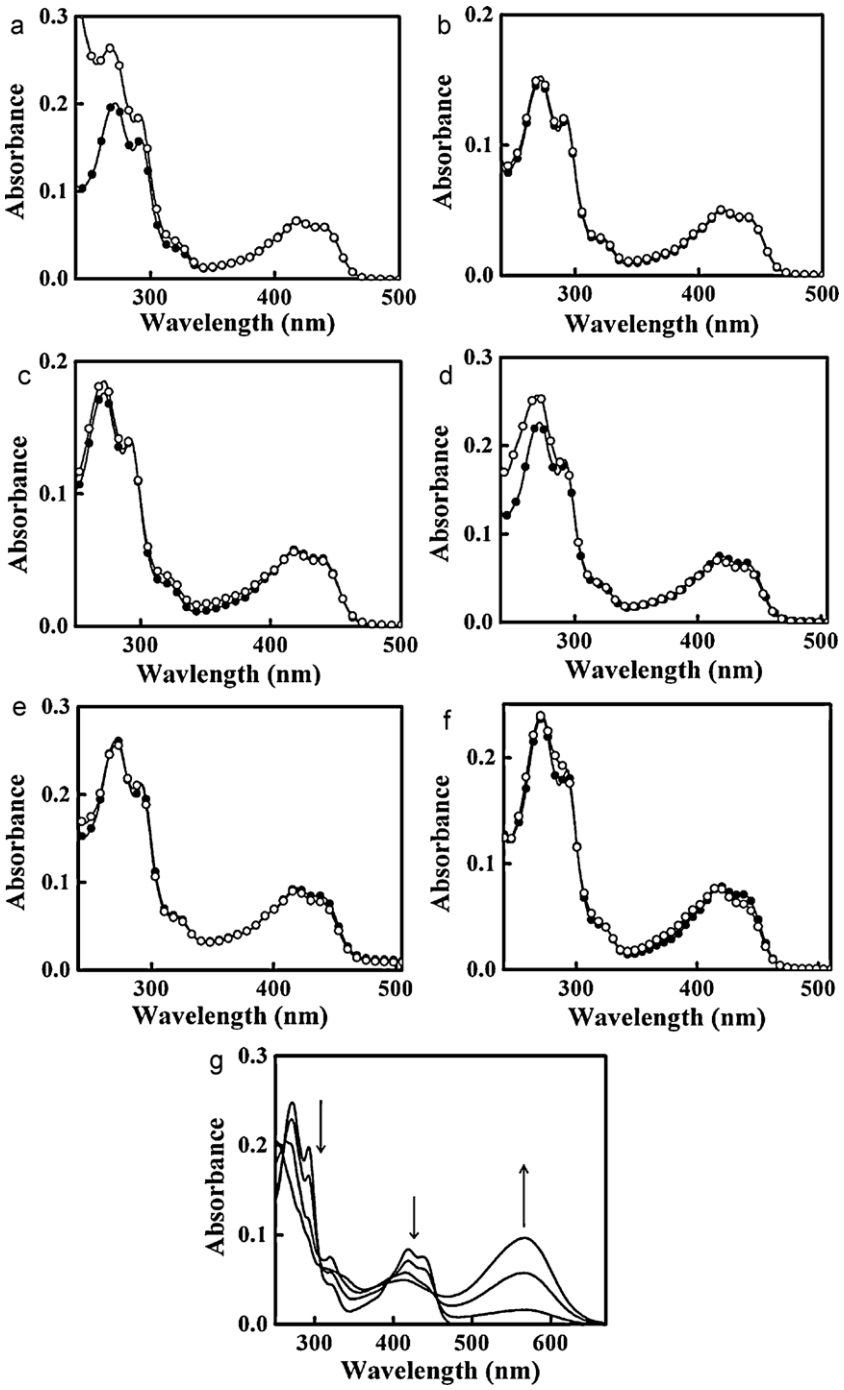

Fig. 3. Absorption spectra of 2N1YMN1O in ACN solvent (-●-) and in the presence of 30 μM of different transition metal ions (-○-) e.g., (a) Cr^{3+}, (b) Mn^{2+}, (c) Fe^{2+}, (d) Co^{2+}, (e) Ni^{2+}, (f) Zn^{2+}; (g) absorption spectra of 2N1YMN1O in the presence of increasing concentration of Cu^{2+} ion. Direction of arrow indicates increasing concentration of Cu^{2+} (0, 6.67, 16.12, 30.01 μM).

be explored on the basis of PET mechanism, which is a commonly exploited strategy for fluorosensors for metal ions showing intensity enhancement [13,15]. In order to substantiate on the postulation, the following series of experiments and arguments have been undertaken.

Firstly, we focus on establishing the efficiency of the studied molecular architecture to function as a suitable system in order for PET mechanism to take place in it. A search for the extent of electron deficiency of the fluorophore unit in 2N1YMN1O has been employed as the actuating yardstick for this purpose [13,15].

3.2.3.1. Redox behaviour. In an attempt to assess the electron deficiency of the fluorophore unit in 2N1YMN1O cyclic voltametric measurements have been performed. The E_{red}(fluoro) appears at −0.962 V (irreversible) while the oxidation potential is observed at E_{ox}(fluoro) = 0.891 V (irreversible). Now, with the measured reduction potential coupled with the spectral data, a quantitative estimate of the thermodynamic driving force for PET process in 2N1YMN1O can be achieved in terms of the free energy change (ΔG) of the process [13,15]. The ΔG value has been calculated using the equation: $\Delta G = 23.06[E_{ox}(\text{recep}) - E_{red}(\text{fluoro})] - E_{0,0}$, in which E_{ox}(recep) is the oxidation potential of the receptor moiety,

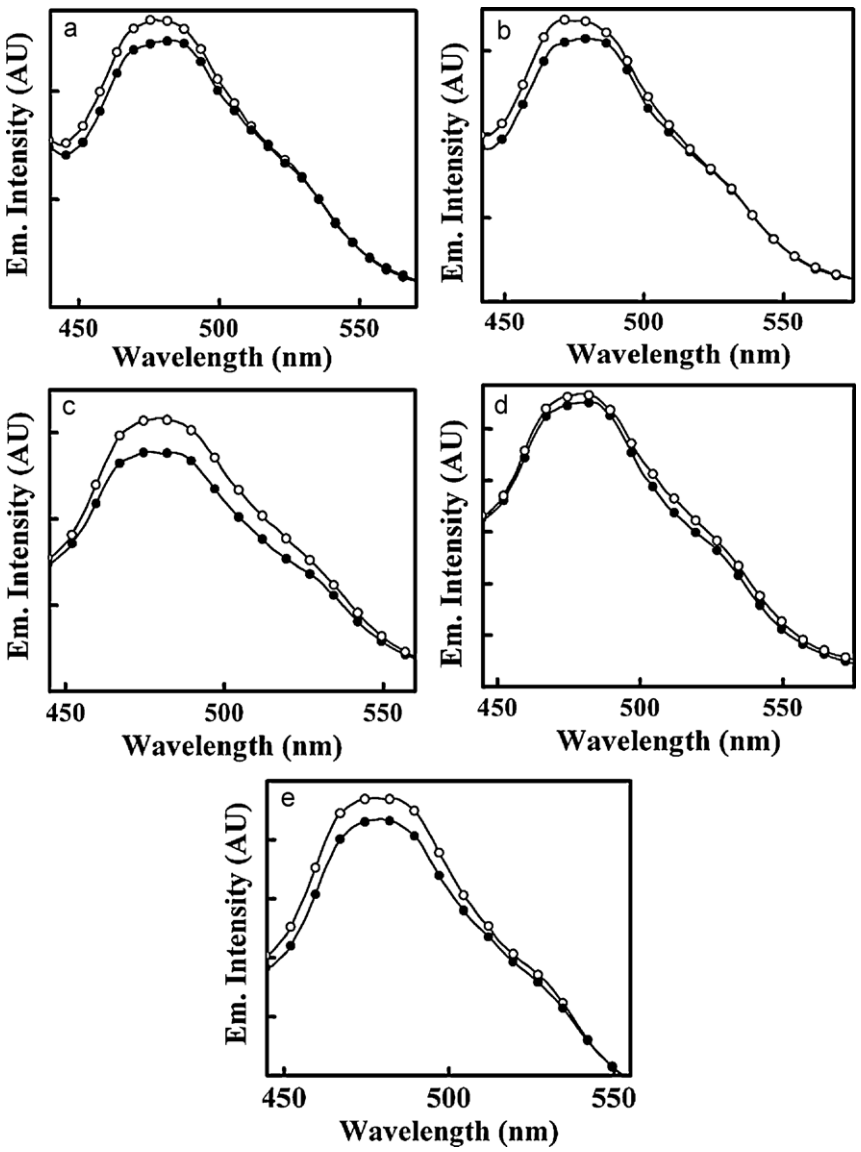

Fig. 4. Emission spectra (λ_{ex} = 430 nm) of 2N1YMN1O in ACN solvent (-●-) and in the presence of 50 μM different transition metal ions (-○-) e.g., (a) Cr^{3+}, (b) Mn^{2+}, (c) Fe^{2+}, (d) Co^{2+}, (e) Ni^{2+}.

E_{red}(fluoro) is the reduction potential of the fluorophore and $E_{0,0}$ represents the energy of the fluorescent state [13,15]. The value of $E_{0,0}$ used in the calculation has been estimated from location of the first peak position in the fluorescence spectrum ($\lambda_{em} \approx 490$ nm). Using E_{ox}(recep) = 0.49 V [13,15] (for triethylamine, literature SCE value corrected for Ag/AgCl electrode by subtracting 0.27 V), ΔG value comes out to be =−24.88 kcal/mol, which dictates the thermodynamic feasibility of the PET process in the studied system.

3.2.3.2. An assessment from fluorescence quantum yield. Another simple and direct way to evaluate the electron deficient character of the fluorophore unit in 2N1YMN1O is to compare its fluorescence quantum yield with that of the constituent compound, HN12 [30]. Table 1 throws glimpse on the factor by which the quantum yields of 2N1YMN1O in various solvents are lower than the value for the parent compound HN12, and the presently investigated compound is found to be, by far an inefficient fluorophore compared to its constituent compound.

3.2.3.3. An assessment from fluorescence quenching behaviour. Initially it is surprising to note a contrasting behaviour of the transition metal ions (Zn^{2+} and Cu^{2+}) resulting in fluorescence enhancement (*vide* Fig. 5), which are usually known for their quenching actions. Herein, we endeavour to answer to the enigma by taking into account the individual interactions operative in the presence and absence of the guest and by comparing the effects for 2N1YMN1O with those on its parent compound, HN12.

The constituent fluorophore HN12 is found to undergo usual quenching as induced by the transition metal ions Zn^{2+} and Cu^{2+}. The extent of quenching has been quantitatively estimated on the Stern–Volmer equation [6,13]:

$$\frac{I_0}{I} = 1 + K_{SV}[Q] = 1 + k_q\tau_0[Q] \quad (4)$$

in which K_{SV} is the Stern–Volmer quenching constant and k_q is the bimolecular quenching constant. I_0 is the original fluorescence intensity, I is the quenched intensity and τ_0 is the excited state fluorescence lifetime of the unquenched fluorophore [13,15]. Cu^{2+} ion (with one unpaired electron) is found to be a more efficient quencher for HN12 than Zn^{2+}, with $K_{SV} = 7.75 \times 10^4\ M^{-1}$ for Cu^{2+} and $1.13 \times 10^3\ M^{-1}$ for Zn^{2+} (correspondingly the bimolecular quenching constant values are $k_q = 7.61 \times 10^{13}\ M^{-1}\ s^{-1}$ for

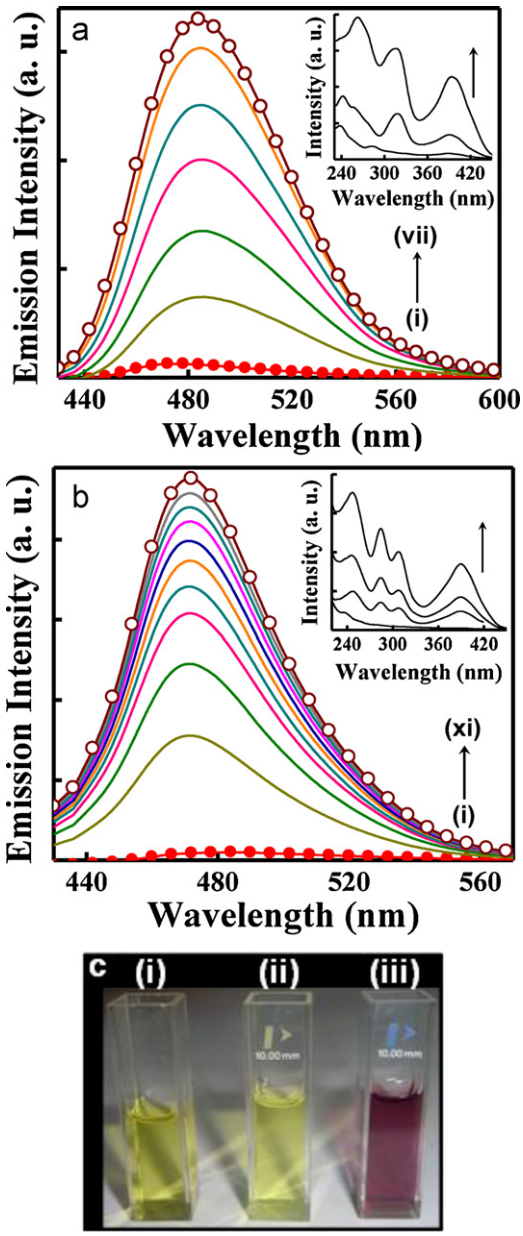

Fig. 5. Emission spectra (λ_{ex} = 365 nm) of 2N1YMN1O in ACN solvent in the presence of increasing concentration of transition metal ions, (a) Cu^{2+} and (b) Zn^{2+}. Inset shows the excitation spectra in the presence of increasing concentration of respective transition metal ions. Curves (i) → (xi) correspond to $[M^{n+}]$ = 0, 6.67, 12.24, 20.01, 26.68, 33.35, 40.02, 46.69, 53.36, 60.03, and 66.7 μM. (c) Photographs of (i) 2N1YMN1O, (ii) 2N1YMN1O + Zn^{2+} and (iii) 2N1YMN1O + Cu^{2+} showing the visual colour change of 2N1YMN1O in the presence of the metal ions.

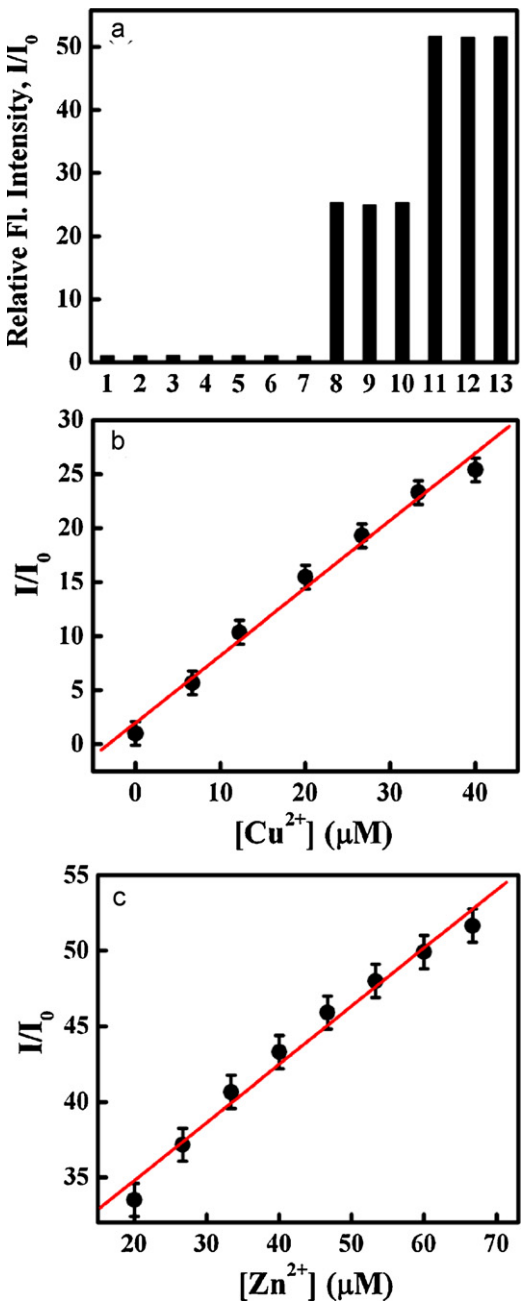

Fig. 6. Ratiometric chemosensory emission spectral response of 2N1YMN1O. (a) Variation of relative emission intensity (I/I_0) of 2N1YMN1O in the presence of different metal ions (1: Cr^{3+}, 2: Mn^{2+}, 3: Fe^{2+}, 4: Co^{2+}, 5: Ni^{2+}, 6: Mg^{2+}, 7: Ca^{2+}, 8: Cu^{2+}, 9: Cu^{2+} + Mg^{2+}, 10: Cu^{2+} + Ca^{2+}, 11: Zn^{2+}, 12: Zn^{2+} + Mg^{2+}, 13: Zn^{2+} + Ca^{2+}) (concentration of each of first row transition metal cation = 55 μM and that of each of alkaline earth cation = 20 μM). (b) The construction of calibration curve for detection of Cu^{2+} (the linear regression follows the equation: $y = 1.965 + 0.624x$) and (c) the construction of calibration curve for detection of Zn^{2+} (the linear regression follows the equation: $y = 27.086 + 0.385x$).

Cu^{2+} and $1.11 \times 10^{12}\ M^{-1}\ s^{-1}$ for Zn^{2+}. $k_q = K_{SV}/\tau_0$ [6,13], where τ_0 (=1.019 ns) is the fluorescence lifetime of HN12 in the absence of quencher [30]). Thus interaction between the fluorophore (naphthalene unit of 2N1YMN1O) and transition metal ions (Cu^{2+} and Zn^{2+}) results in fluorescence quenching, whereas that between the receptor (imine moiety of 2N1YMN1O) and the metal ions leads to fluorescence enhancement. Hence it is presumed that it is the net result of this two opposing interactions that will play the governing role behind the resultant consequence (quenching or enhancement) of interaction of 2N1YMN1O with the transition metal ions (Cu^{2+} and Zn^{2+}).

Since the fluorescence yield of 2N1YMN1O is very low (*vide* Table 1) in the absence of the guest (reflecting the presence of a communication (PET) between the flurophore and the receptor resulting in decreasing the fluorescence yield of the compound), it is not unlikely that the interaction with the guest counterpart will lead to modulation of the fluorophore–receptor communication in a manner that facilitates fluorescence enhancement (by turning OFF or impairing the fluorophore–receptor communication). This proposition is supported by the results of redox behaviour of 2N1YMN1O and the comparative assessment of its fluorescence yield with that of the parent compound HN12, as dis-

cussed above, and also is in consensus with available literature reports [13,15].

3.2.3.4. Time-resolved fluorescence decay behaviour. Fluorescence lifetime measurements often serve as a sensitive indicator of the local environment of a fluorophore, and it is responsive to excited state affairs [13,15,35,36]. Thus in order to achieve a deeper insight into the photophysics of 2N1YMN1O and its modulation in the presence of transition metal ions, fluorescence lifetimes have been monitored under differential circumstances. Fig. 7 depicts the time-resolved fluorescence decay profile of 2N1YMN1O under varied experimental conditions and the relevant data are compiled in Table 2. The decay behaviour of either the bare fluorophore or its metal complex is found to be complicated and is best fitted to bi and triexponential functions.

With a view to the complicated absorption profile of 2N1YMN1O in different solvents (*vide* Fig. 1) the decay characteristics have been monitored at λ_{ex} = 340 nm in MCH and λ_{ex} = 405 nm in ACN and MeOH (Fig. 7a and Table 2). It is interesting to note that the complicated triexponential decay pattern of 2N1YMN1O reflects the presence of a short-lived major component (~9.6 ps, 99% in ACN), which seems to be a representative of the lifetime of PET-quenched fluorophore [13,15,35]. The long-lived minor components may in principle emanate from the products of electron transfer reactions such as an exciplex. However, the absence of any fluorescence peak of 2N1YMN1O at longer wavelengths and the high dielectric constant of the medium (ACN, ε = 37.5; where exciplexes are unstable) leads to negate this possibility [13,15]. Further reinforcing support in favour of negation of the possibility of exciplex formation comes from a similar fluorescence decay pattern observed in non-polar solvent MCH (Fig. 7a and Table 2). The triexponential nature of the fluorescence decay can be explained by a through space electron-transfer mechanism involving the overlap of the lone pair orbital of the distal nitrogen and the π-orbitals of the ring. The long-lived components arise from species in which the donor and acceptor groups are well separated, while the predominant short-lived component represents the quenched fluorophore having the donor imine in close proximity [13,15,35].

The overall decay behaviour of 2N1YMN1O in the presence of transition metal ions is seen to undergo noticeable modification (Fig. 7b and Table 2) though the complicacy persists and it becomes even more cumbersome to explain the observations by placing equal emphasis on each decay component. Thus instead of placing too much importance on individual decay components the average (mean) fluorescence lifetimes ($\langle\tau_f\rangle$) have been calculated (Table 2) and the observations are found to corroborate to the steady-state findings. In the presence of Zn^{2+} ion the decay is seen to be rendered clearly biexponential, while with Cu^{2+} ion the basic complicacy persists. However, an overall increase of the average fluorescence lifetime imparted by the presence of both the transition metal ions is distinctly detectable (Table 2). In order to delineate the effect, a more crucial analysis of the data has been endevoured with a view to delineate the contributions from radiative (k_r) and nonradiative (k_{nr}) decay rate constants according to the following equations [13]:

$$k_r = \frac{\langle\tau_f\rangle}{\Phi_f} \tag{5}$$

$$k_r + k_{nr} = \langle\tau_f\rangle^{-1} \tag{6}$$

and the calculated results are summarized in Table 3. A careful examination of the data (Table 3) reveals that interaction of 2N1YMN1O with the transition metal ions results in depletion of nonradiative decay rates but only nominally, while a marked enhancement of the radiative decay rates appears to play the pivotal role behind the observed fluorescence enhancement (*vide* Fig. 5). Though it is obvious that a sort of binding interaction of 2N1YMN1O with the transition metal ion would impart rigidity to the entire molecular framework whereby reducing the rotation/vibrational degrees of freedom and hence contributing to fluorescence enhancement, this explanation does not seem to suffice for the magnitude of the observed enhancement. Furthermore, time-resolve fluorescence decays clearly show the presence of PET-quenched components. Thus it appears that transition cation-induced perturbation of PET in the multicomponent system, 2N1YMN1O marks its signature in fluorescence enhancement more prominently through increase of radiative rates than reduction of nonradiative rates.

A simplified design-schematic for the transition metal ion-induced fluorescence enhancement of 2N1YMN1O through perturbation of the PET process is summarized in Scheme 2.

It could be pertinent at this stage to compare between Cu^{2+} and Zn^{2+} for the proposed mechanism (perturbation of PET) resulting in observed emission enhancement of 2N1YMN1O. The time-resolved fluorescence decay characteristics for 2N1YMN1O in various environments as compiled in Table 2 can be employed to provide an insight into the matter. The data (Table 2) show evidence for Cu^{2+} ion-induced perturbation of PET in 2N1YMN1O through impairing the short-lived major component of fluorescence decay which is representative of PET-quenched fluorophore. However, the presence of Zn^{2+} is found to impart perturbation of PET in 2N1YMN1O to a much greater extent. This comparison is further substantiated from the observation reported in Fig. 6 which shows that in the presence of the same concentration (55 μM) of the metal ions (Cu^{2+} or Zn^{2+}) fluorescence enhancement in 2N1YMN1O occurs to a significantly greater extent for Zn^{2+}. This could be related to the greater binding efficiency of 2N1YMN1O with Zn^{2+} than Cu^{2+} (to be discussed in forthcoming section).

3.3. Strength of 2N1YMN1O – metal ion interaction and the probable functional groups of 2N1YMN1O involved in the interaction

The foregoing discussions reveal the occurrence of interaction of the multicomponent system (2N1YMN1O) with the respective guest counterparts (Cu^{2+} and Zn^{2+} ions) and the consequence of this interaction is manifested on the modulated photophysics of 2N1YMN1O as imparted by the guest. Herein, we endeavour to estimate the strength of the interaction in terms of determination of the binding constant (K) [35]. An assessment of the emission intensity data on modified Benesi–Hildebrand equation has been exploited for the said purpose. A detailed discussion on Benesi–Hildebrand equation is avoided since it is routine and profusely available in the literature [36]. We thus start with the equation [13,36,37]:

$$\frac{1}{(I - I_0)} = \frac{1}{(I_1 - I_0)} + \frac{1}{(I_1 - I_0)K[M^{n+}]} \tag{7}$$

in which I_0, I and I_1 are the emission intensities, respectively, in the absence of, at intermediate and infinite concentration of the metal ion (M^{n+}).

A linear regression for the plot of $[I - I_0]^{-1}$ vs. $[M^{n+}]^{-1}$ is obtained for both Cu^{2+} and Zn^{2+} ions (Fig. 8) and the binding constant is evaluated as K = intercept to slope ratio of the plot = $(4.95 \pm 1.2) \times 10^4\ M^{-1}$ for Zn^{2+} and $(1.48 \pm 1.2) \times 10^3\ M^{-1}$ for Cu^{2+}. Hence the corresponding free energy change is $\Delta G = -RTlnK = -26.96$ kJ/mol for Zn^{2+} and -18.21 kJ/mol for Cu^{2+}, i.e. a negative free energy change dictates the thermodynamic feasibility for the occurrence of the binding interaction between the two parties (2N1YMN1O and the guest counterpart).

It is pertinent at this point to make an effort to unveil the functional groups of 2N1YMN1O that are involved in the interaction with the transition metal ions. The ^1H NMR spectroscopic technique has been explored for this purpose. Fig. 9 displays the ^1H

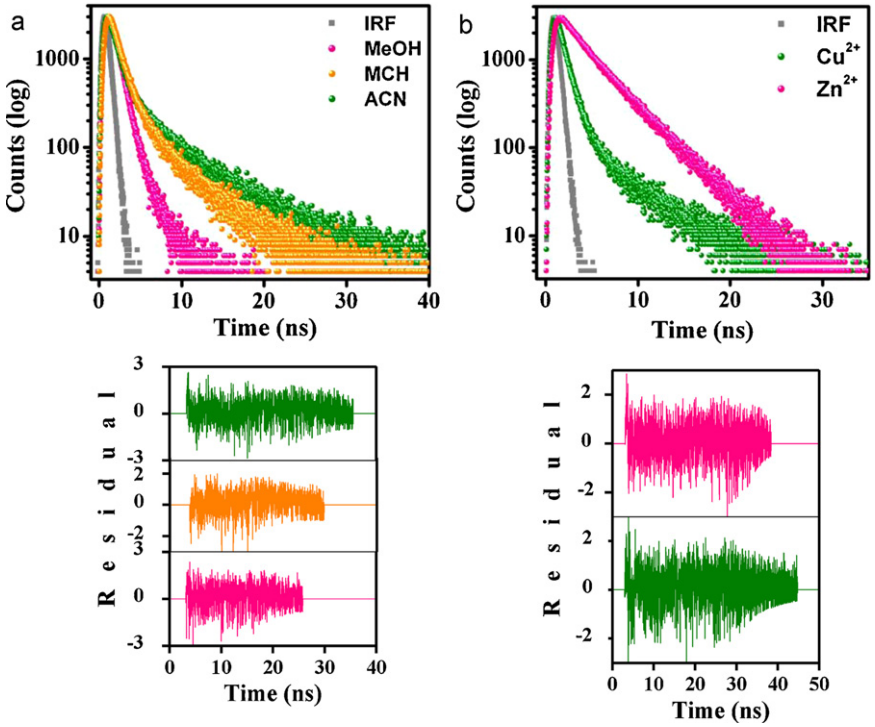

Fig. 7. Typical time-resolved fluorescence decay profile of 2N1YMN1O (a) in various solvents as indicated in the figure legend and (b) in the presence of 30 μM each of Cu^{2+} and Zn^{2+} ions in ACN solvent. The lower panel shows the residual plot for the respective fitted functions to the actual data.

Table 2
Time-resolved fluorescence decay parameters of 2N1YMN1O in different environments.

Environment	τ_1 (ns)	τ_2 (ns)	τ_3 (ps)	α_1	α_2	α_3	$\langle\tau_f\rangle$ (ns)	χ^2
MCH	0.79	2.28	–	0.95	0.05	–	0.99	0.98
ACN	0.88	4.51	9.6	0.012	1.73×10^{-3}	0.99	1.6	0.99
MeOH	0.86	4.014	11.7	6.24×10^{-4}	3.05×10^{-4}	0.99	0.41	1.02
[a]Cu^{2+}	0.86	6.15	26	7.66×10^{-3}	3.07×10^{-3}	0.98	2.39	1.01
[a]Zn^{2+}	1.63	4.004	–	0.32	0.68	–	3.62	1.00

[a] In the presence of 30 μM metal ion in ACN.

Table 3
Fluorescence quantum yield (Φ_f) and kinetic fluorometric and nonradiative parameters for 2N1YMN1O in the presence and absence of transition metal ions in ACN solvent.

Environment	Φ_f	$\langle\tau_f\rangle$ (ns)	k_r (s^{-1})	k_{nr} (s^{-1})
ACN	0.098×10^{-2}	1.6	6.13×10^5	6.24×10^8
Zn^{2+}	0.244	3.62	6.74×10^7	2.09×10^8
Cu^{2+}	0.107	2.39	4.49×10^7	3.74×10^8

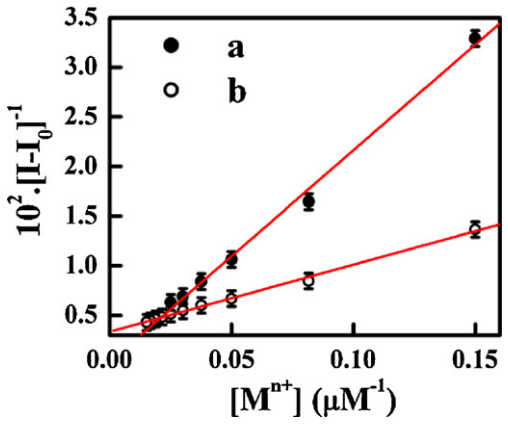

Fig. 8. Benesi–Hildebrand plot ($[I - I_0]^{-1}$ vs. $[M^{n+}]^{-1}$) for complexation between 2N1YMN1O and the transition metal ions ((a) Cu^{2+} and (b) Zn^{2+}), derived from emission spectral data.

NMR spectral profiles of 2N1YMN1O in the absence and presence of Zn^{2+} (for reasons of compatible solubility of both the compound 2N1YMN1O and the perchlorate salt of the metal ion the ^1H NMR spectra in Fig. 9 are recorded in a mixture of $CDCl_3$ and DMSO-d_6). Though the ^1H NMR spectra of 2N1YMN1O is not found to exhibit drastically large modifications of chemical shift upon interaction with Zn^{2+}, some discernible modifications can be noted. The presence of Zn^{2+} ion is found to induce an upfield shift to the OH proton (δ 13.42–13.4) and the =N–CH_2– proton (δ 5.26–5.24). It was difficult to distinctly point out the shifting in the –CH=N– proton because of the splitting of its signal into multiplet [38]. This finding probably points at the involvement of the OH functional moiety and the imine centre in 2N1YMN1O in the interaction with Zn^{2+} ion [38]. The protons in the remote part of the molecular framework from the site of interaction do not experience notable change in chemical shift. However, in order to deduce a more pinpointing inference on the issue the X-ray crystallographic structure elucidation of the 2N1YMN1O–M^{n+} complex system should have been a more appropriate candidate. Unfortunately we refrain from the

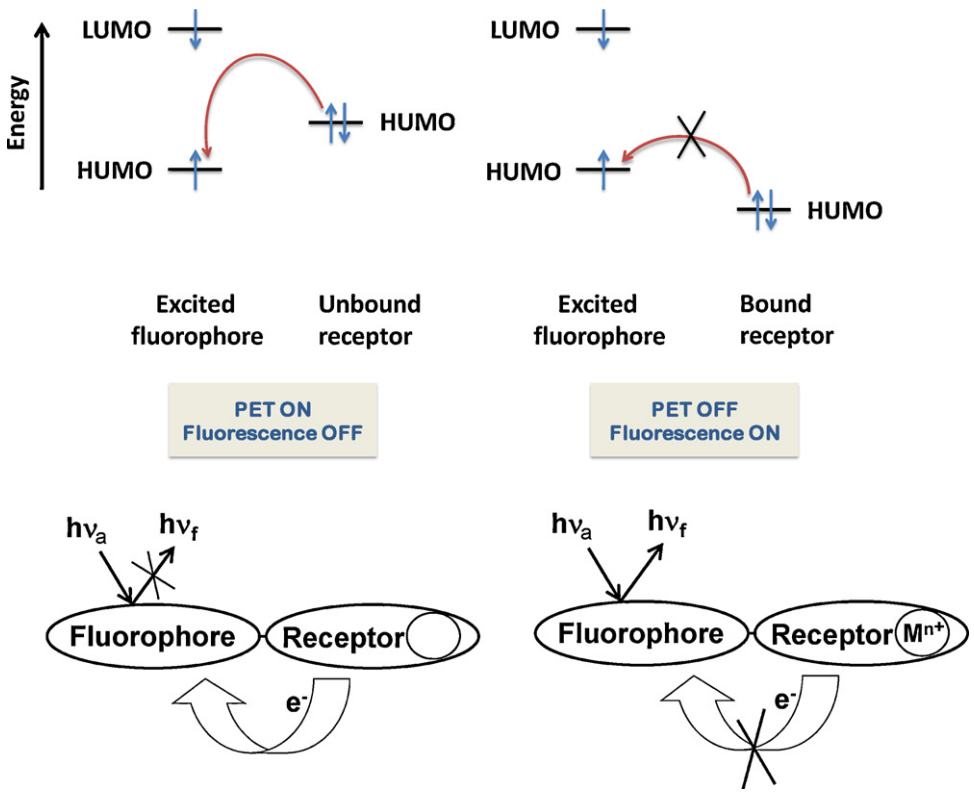

Scheme 2. A simplified design-schematic for the transition metal ion-induced fluorescence enhancement of 2N1YMN1O through perturbation of the PET process.

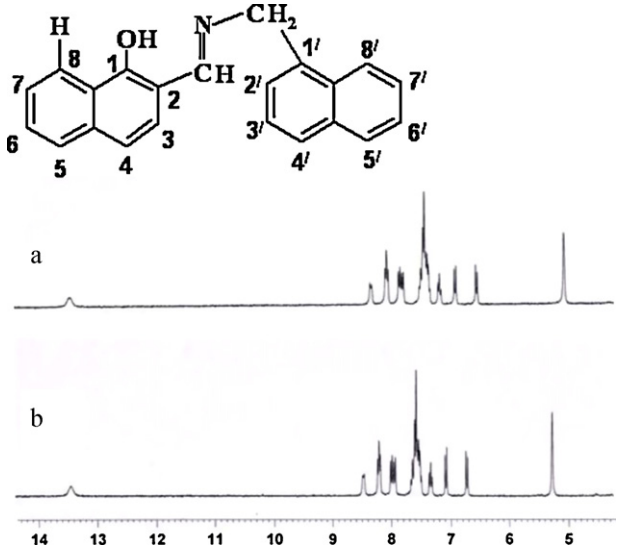

Fig. 9. ^{1}H NMR spectra of 2N1YMN1O in the (a) absence and (b) presence of Zn^{2+}.

issue since even after our repeated attempts the quality of the crystal of the 2N1YMN1O–M^{n+} complex system was not suitable for X-ray crystallographic structure analysis.

4. Conclusion

A Schiff base-derived new model compound, 2N1YMN1O has been synthesized and its photophysics has been characterized by steady-state absorption, emission and time-resolved emission spectroscopic techniques. Originally the fluorescence yield of the compound is found to be considerably low compared to its constituent compound, HN12. This has been rationalized in connection with the operation of PET mechanism from the imine moiety to the fluorophore unit in the multicomponent system, 2N1YMN1O. The transition metal ion-induced modulations of the fluorescence properties of 2N1YMN1O unravel significant fluorescence enhancement in the presence of Cu^{2+} and Zn^{2+} ions selectively. Hence, 2N1YMN1O has subsequently been argued to be a promising candidate for the development of Cu^{2+} and Zn^{2+} ion selective fluorescence chemosensor with particular emphasis on its ratiometric chemosensory function and the construction of a calibration curve for the estimation of the transition metal ions in an unknown sample down to the limit of micromolar concentration. The ratiometric chemosensory caliber of 2N1YMN1O has been established on the lexicon of a detailed assessment over the range of first row transition cations and alkaline earth cations. As such the mechanism of fluorescence enhancement has been intertwined with perturbation of Cu^{2+}/Zn^{2+} ion-induced PET in 2N1YMN1O and the selectivity for these two transition metal ions can be connected to the appreciable strength of interaction with these metal ions compared to others. Additional edges of 2N1YMN1O to function as a fluorescence chemosensor are its relatively simple structure and simple synthetic route. Also such commendable selectivity in generating sensing responses indicates the possibility of viable expansion of the technique to further consequences in sensory research.

Acknowledgements

B.K.P. gratefully acknowledges C.S.I.R., India for a research fellowship. N.G. acknowledges D.S.T., India (Project no. SR/S1/PC/26/2008) for financial support. The authors greatly appreciate the cooperation received from Professor Dr. T. Ganguly and Mr. S. Das of Spectroscopy Department, IACS, India for fluorescence lifetime measurements. The authors gratefully acknowledge the anonymous reviewers for their meticulous inspection of the work and very constructive suggestions.

Appendix A. Supplementary data

Supplementary data associated with this article can be found, in the online version, at doi:10.1016/j.jphotochem.2011.04.006.

References

[1] A.P. de Silva, H.Q.N. Gunaratne, T. Gunnlagsson, A.J.M. Huxley, C.P. McCoy, J.T. Rademacher, T.E. Rice, Signaling recognition events with fluorescent sensors and switches, Chem. Rev. 97 (1997) 1515–1566.

[2] G. Pace, V. Ferri, C. Grave, M. Elbing, C. von Hanisch, M. Zharnikov, M. Mayor, M.A. Rampi, P. Samori, Cooperative light-induced molecular movements of highly ordered azobenzene self-assembled monolayers, Proc. Natl. Acad. Sci. U.S.A. 104 (2007) 9937–9942.

[3] R.A. Bissel, A.P. de Silva, H.Q.N. Gunaratne, P.L.M. Lynch, G.E.M. Maguire, R.A.S. Sandanayake, Molecular fluorescent signalling with 'fluor–spacer–receptor' systems: approaches to sensing and switching devices *via* supramolecular photophysics, Chem. Soc. Rev. 21 (1992) 187–195.

[4] A.W. Czarnik, Chemical communication in water using fluorescent chemosensors, Acc. Chem. Res. 27 (1994) 302–308.

[5] A.W. Czarnik (Ed.), Fluorescent Chemosensors for Ions and Molecule Recognition, American Chemical Society, Washington, DC, 1993.

[6] A.W. Czarnik, in: J.R. Lakowicz (Ed.), Topics in Fluorescence Spectroscopy, vol. 4, Plenum, New York, 1994.

[7] B. Valeur, in: J.R. Lakowicz (Ed.), Topics in Fluorescence Spectroscopy, vol. 4, Plenum, New York, 1994.

[8] F.L. Carter, R.E. Siatkowski, H. Wohltjen (Eds.), Molecular Electronic Devices, Elsevier, Amsterdam, 1988.

[9] J.M. Lehn, Supramolecular chemistry—scope and perspectives molecules, supermolecules, and molecular devices (Nobel Lecture), Angew. Chem. Int. Ed. Engl. 27 (1988) 89–112.

[10] J.M. Lehn, Perspectives in supramolecular chemistry—from molecular recognition towards molecular information processing and self-organization, Angew. Chem. Int. Ed. Engl. 29 (1990) 1304–1319.

[11] J.M. Lehn, Supramolecular Chemistry, VCH, Weinheim, 1995.

[12] A.P. de Silva, D.B. Fox, T.S. Moody, S.M. Weir, The development of molecular fluorescent switches, Trends Biotechnol. 19 (2001) 29–34.

[13] J.R. Lakowicz, Principles of Fluorescence Spectroscopy, Plenum, New York, 1999.

[14] Z. Xu, K.-H. Baek, H.N. Kim, J. Cui, X. Qian, D.R. Spring, I. Shin, J. Yoon, Zn^{2+}-triggered amide tautomerization produces a highly Zn^{2+}-selective, cell-permeable, and ratiometric fluorescent sensor, J. Am. Chem. Soc. 132 (2010) 601–610.

[15] B. Ramachandram, G. Saroja, N.B. Sankaran, A. Samanta, Unusually high fluorescence enhancement of some 1,8-naphthalimide derivatives induced by transition metal salts, J. Phys. Chem. B 104 (2000) 11824–11832.

[16] T. Glunnlaugsson, J.P. Leonard, N.S. Murray, Highly selective colorimetric naked-eye Cu(II) detection using an azobenzene chemosensor, Org. Lett. 6 (2004) 1557–1560.

[17] X.-L. Tang, X.-H. Peng, W. Dou, J. Mao, J.-R. Zheng, W.-W. Qin, W.-S. Liu, J. Chang, X.-J. Yao, Design of a semirigid molecule as a selective fluorescent chemosensor for recognition of Cd(II), Org. Lett. 10 (2008) 3653–3656.

[18] T. Hirano, K. Kikuchi, Y. Urano, T. Higuchi, T. Nagano, Highly zinc-selective fluorescent sensor molecules suitable for biological applications, J. Am. Chem. Soc. 122 (2000) 12399–12400.

[19] V.B. Bojinov, I.P. Panova, J.-M. Chovelon, Novel blue emitting tetra- and pentamethylpiperidin-4-yloxy-1,8-naphthalimides as photoinduced electron transfer based sensors for transition metal ions and protons, Sens. Actuators B: Chem. 135 (2008) 172–180.

[20] N. Aksuner, E. Henden, I. Yilmaz, A. Cukurovali, A highly sensitive and selective fluorescent sensor for the determination of copper(II) based on a Schiff base, Dyes Pigments 83 (2009) 211–217.

[21] D. Tuan Quang, J.S. Kim, Fluoro- and c hromogenic chemodosimeters for heavy metal ion detection in solution and biospecimens, Chem. Rev. 110 (2010) 6280–6301.

[22] K. Eiichi, T. Koike, Recent development of zinc-fluorophores, Chem. Soc. Rev. 27 (1998) 179–184.

[23] U.E. Spichiger-Keller, Chemical Sensors and Biosensors for Medical and Biological Applications, Wiley-VCH, Berlin, 1998.

[24] C.J. Frederickson, J.-Y. Koh, A.I. Bush, The neurobiology of zinc in health and disease, Nat. Rev. Neurosci. 6 (2005) 449–462.

[25] P.J. Fraker, L.E. King, Reprogramming of the immune system during zinc deficiency, Annu. Rev. Nutr. 24 (2004) 277–298.

[26] J.W. Buck, D.A. Tolle, G. Whelan, T.J. Mast, M.S. Peffers, P.G. Georgopoulos, S.W. Wang, P.J. Lioy, I.G. Georgopoulos, M.J. Yononne-Lioy, Assessment of human exposure to copper: a case study using the NHEXAS database, J. Expo. Sci. Environ. Epidemiol. 16 (2006) 397–409.

[27] A.F. Cahudhry, M. Verma, M.T. Morgan, M.M. Henary, N. Siegel, J.M. Hales, J.W. Perry, C.J. Fahrni, Kinetically controlled photoinduced electron transfer switching in Cu(I)-responsive fluorescent probes, J. Am. Chem. Soc. 132 (2010) 737–747.

[28] M. Taki, S. Iyoshi, A. Ojida, I. Hamachi, Y. Yamamoto, Development of highly sensitive fluorescent probes for detection of intracellular copper(I) in living systems, J. Am. Chem. Soc. 132 (2010) 5938–5939.

[29] C. Reichardt, Solvents and Solvent Effects in Organic Chemistry, VCH, Weinheim, 1988 (chapter 7).

[30] R.B. Sing, S. Mahanta, S. Kar, N. Guchhait, Photo-physical properties of 1-hydroxy-2-naphthaldehyde: a combined fluorescence spectroscopy and quantum chemical calculations, Chem. Phys. 331 (2007) 373–384.

[31] S.R. Vazquez, M.C.R. Rodriguez, M. Mosquera, F. Rodriguez-Prieto, Excited-state intramolecular proton transfer in 2-(3′-hydroxy-2′-pyridyl)benzoxazole. Evidence of coupled proton and charge transfer in the excited state of some *o*-hydroxyarylbenzazoles, J. Phys. Chem. A 111 (2007) 1814–1826.

[32] C. Rodriguez-Rodriguez, N.S. de Groot, A. Rimola, A. Alvarez-Larena, V. Lloveras, J. Vidal-Gancedo, S. Ventura, J. Vendrell, M. Sodupe, P. Gonzalez-Duarte, Design, selection, and characterization of thioflavin-based intercalation compounds with metal chelating properties for application in alzheimer's disease, J. Am. Chem. Soc. 131 (2009) 1436–1451.

[33] W.-H. Chen, Y. Pang, Excited-state intramolecular proton transfer in 2-(2′,6′-dihydroxyphenyl)benzoxazole: effect of dual hydrogen bonding on the optical properties, Tetrahedron Lett. 51 (2010) 1914–1918.

[34] W. Turbeville, P.K. Dutta, Spectroscopic studies of the photochromic molecule N-(2-hydroxybenzylidene)aniline and its photoproduct, J. Phys. Chem. A 94 (1990) 4060–4066.

[35] K. Sarkar, K. Dhara, M. Nandi, P. Roy, A. Bhaumik, P. Banerjee, Selective zinc(II)-ion fluorescence sensing by a functionalized mesoporous material covalently grafted with a fluorescent chromophore and consequent biological applications, Adv. Funct. Mater. 19 (2009) 223–234.

[36] B.K. Paul, N. Guchhait, Modulated photophysics of an ESIPT probe 1-hydroxy-2-naphthaldehyde within motionally restricted environments of liposome membranes having varying surface charges, J. Phys. Chem. B 114 (2010) 12528–12540.

[37] H.A. Benesi, J.H. Hildebrand, A spectrophotometric investigation of the interaction of iodine with aromatic hydrocarbons, J. Am. Chem. Soc. 71 (1949) 2703–2707.

[38] Z. Xu, S. Kim, K.-H. Lee, Y. Yoon, A highly selective fluorescent chemosensor for dihydrogen phosphate via unique excimer formation and PET mechanism, Tetrahedron Lett. 48 (2007) 3797–3800.